THE JOURNAL OF BIOLOGICAL CHEMISTRY VOL. 287, NO. 9, pp. 6725–6734, February 24, 2012


# Dimeric α-Cobratoxin X-ray Structure

## *LOCALIZATION OF INTERMOLECULAR DISULFIDES AND POSSIBLE MODE OF BINDING TO NICOTINIC ACETYLCHOLINE RECEPTORS**

Received for publication, November 11, 2011, and in revised form, December 22, 2011 Published, JBC Papers in Press, January 5, 2012, DOI 10.1074/jbc.M111.322313

**Alexey V. Osipov[‡1], Prakash Rucktooa[§1,2], Igor E. Kasheverov[‡¶], Sergey Yu. Filkin[‡], Vladislav G. Starkov[‡], Tatyana V. Andreeva[‡], Titia K. Sixma[§], Daniel Bertrand[‖], Yuri N. Utkin[‡¶], and Victor I. Tsetlin[‡3]**

*From the [‡]Shemyakin-Ovchinnikov Institute of Bioorganic Chemistry, Russian Academy of Sciences, ul. Miklukho-Maklaya 16/10, Moscow 117997, Russia, the [§]Division of Biochemistry and Center for Biomedical Genetics, The Netherlands Cancer Institute, Plesmanlaan 121, 1066 CX Amsterdam, The Netherlands, [¶]Syneuro, ul. Miklukho-Maklaya 16/10, Moscow 117997, Russia, and [‖]HiQScreen, 15 rue de l'Athénée, 1206 Geneva, Switzerland*

**Background:** α-Cobratoxin (αCT) dimer (αCT-αCT) has recently been discovered and found to bind both with α7 and α3β2 nicotinic receptors (nAChR).
**Results:** αCT-αCT x-ray structure and intermolecular disulfides were established, intramolecular disulfides in central loops II were reduced, and interaction with distinct nAChRs was analyzed.
**Conclusion:** Loop II disulfide is necessary for αCT-αCT binding to α7 but not α3β2 nAChR.
**Significance:** Dimeric α-neurotoxins provide new means for distinguishing distinct nAChRs.

**In *Naja kaouthia* cobra venom, we have earlier discovered a covalent dimeric form of α-cobratoxin (αCT-αCT) with two intermolecular disulfides, but we could not determine their positions. Here, we report the αCT-αCT crystal structure at 1.94 Å where intermolecular disulfides are identified between Cys[3] in one protomer and Cys[20] of the second, and vice versa. All remaining intramolecular disulfides, including the additional bridge between Cys[26] and Cys[30] in the central loops II, have the same positions as in monomeric α-cobratoxin. The three-finger fold is essentially preserved in each protomer, but the arrangement of the αCT-αCT dimer differs from those of noncovalent crystallographic dimers of three-finger toxins (TFT) or from the κ-bungarotoxin solution structure. Selective reduction of Cys[26]-Cys[30] in one protomer does not affect the activity against the α7 nicotinic acetylcholine receptor (nAChR), whereas its reduction in both protomers almost prevents α7 nAChR recognition. On the contrary, reduction of one or both Cys[26]-Cys[30] disulfides in αCT-αCT considerably potentiates inhibition of the α3β2 nAChR by the toxin. The heteromeric dimer of α-cobratoxin and cytotoxin has an activity similar to that of αCT-αCT against the α7 nAChR and is more active against α3β2 nAChRs. Our results demonstrate that at least one Cys[26]-Cys[30] disulfide in covalent TFT dimers, similar to the monomeric TFTs, is essential for their recognition by α7 nAChR, although it is less important for interaction of covalent TFT dimers with the α3β2 nAChR.**

Nicotinic acetylcholine receptors (nAChRs)[4] are among the most thoroughly investigated ligand-gated ion channels. There are two main groups of nAChRs: muscle-type and neuronal receptors. Muscle-type nAChRs consist of five subunits (two α1, one β1, one γ (or ε), and one δ subunit) and contain two binding sites for agonists/competitive antagonists that are located at the interfaces of two α subunits with the adjacent γ and δ subunits. Neuronal nAChRs consist of subunits of two different types: α (α2–α10) and β (β2–β4), and are hetero- (formed by different combinations of α and β subunits) or homo- (formed by α subunits of α7–α10 subtypes) pentameric proteins (for review, see Ref. 1). It has recently been shown that neuronal nAChRs are also present in nonneuronal cells, for example in the immune system, where they play an important role in the regulation of inflammation processes (2). Elucidating the roles of different nAChR subtypes requires fine and precise biochemical tools to discriminate among different receptor activities. Toward this end, α-neurotoxins from snake venoms have proven to be valuable instruments. These α-neurotoxins belong to the family of so-called three-finger toxins (TFTs). Three protruding loops (fingers) of their polypeptide chain are fastened by four conserved disulfide bridges, strengthening the core of the molecule, thus forming a "three-finger" spatial motif. α-Neurotoxins interact with nAChRs through their loops and can discriminate between different nAChR subtypes. So-called short chain α-neurotoxins (59–63 amino acid residues, four disulfide bridges) block only muscle-type nAChRs whereas the long chain α-neurotoxins (66–74 residues, with an additional disulfide bond within the central loop II) display an expanded target choice by also blocking the homopentameric

* This work was supported by Neurocypres EU FP7 Program Grant 202033, Russian Ministry of Education and Science Contract 02.740.11.0865, Russian Foundation for Basic Research Grants 09-04-01061, 10-04-00708, and 11-04-01011 as well as the Molecular and Cell Biology Program of the Russian Academy of Sciences.

*The atomic coordinates and structure factors (code 4AEA) have been deposited in the Protein Data Bank, Research Collaboratory for Structural Bioinformatics, Rutgers University, New Brunswick, NJ (http://www.rcsb.org/).*

[1] Both authors contributed equally to this work.

[2] Supported by a long term European Molecular Biology Organization fellowship.

[3] To whom correspondence should be addressed. Tel./Fax: 007-495-3355733; E-mail: vits@mx.ibch.ru.

[4] The abbreviations used are: nAChR, nicotinic acetylcholine receptor; TFT, three-finger toxin; αCT, α-cobratoxin; AChBP, acetylcholine-binding protein; αCT-αCT, disulfide-bound dimer of α-cobratoxin; αCT-αCT-2AE, α-cobratoxin dimer with one reduced and aminoethylated disulfide bond; αCT-αCT-4AE, α-cobratoxin dimer with two reduced and aminoethylated disulfide bonds; αCT-CTX, disulfide-bound dimer, composed of α-cobratoxin and cytotoxin 3; *Ls*AChBP, *L. stagnalis* AChBP; PDB, Protein Data Bank.

α7 subtype nAChR (3, 4). This additional disulfide bridge in loop II is crucial for the interaction with the homopentameric α7 nAChR. To date, however, neither short nor long chain α-neurotoxins have been shown to block heteropentameric neuronal nAChRs. TFTs from another group, namely κ-bungarotoxins, are able to block heteropentameric α3β2 nAChRs and, to a lesser extent, α4β2 and α7 nAChRs. Structurally, they resemble long chain α-neurotoxins, but they have been characterized as noncovalent dimers based on solution or crystal structures (5). Another group of TFTs, known as weak or nonconventional neurotoxins, comprising 62–68 amino acid residues and five disulfide bridges, has also been described in the literature. The main structural feature of these nonconventional toxins is the presence of a fifth disulfide bridge in the N-terminal loop I. These toxins interact with the α7 and muscle-type nAChRs as well as with muscarinic acetylcholine receptors (6).

Recently, we have isolated a disulfide-bound dimer (αCT-αCT) of α-cobratoxin (αCT), a long chain neurotoxin, from the *Naja kaouthia* cobra venom (7). The peculiarity of this dimer is its capability to block heteropentameric α3β2 nAChRs, in addition to blocking muscle-type and α7 nAChRs, whereas monomeric αCT is not effective against α3β2 nAChRs. We could not establish by chemical means the positions of interchain disulfides in the αCT-αCT dimer. In addition, although the circular dichroism data suggested the preservation of the three-finger fold, in agreement with more or less preserved activity against distinct nAChR subtypes (1), no reliable conclusions could be drawn about the relative spatial disposition of the protomers, and a reliable three-dimensional model of the covalent αCT-αCT dimer could not be generated.

Here, we describe crystallization and the x-ray structure of the αCT-αCT dimer which provides information on the disposition of the intermolecular disulfide bridges, the conformation of protomers, and their assembly into a dimeric neurotoxin. To study the relationship between the structures and the binding modes of monomeric and dimeric αCTs, we modified the αCT-αCT by selectively reducing the additional disulfide bond in loop II ($Cys^{26}$-$Cys^{30}$) either in one or in both protomers and tested the biological activity of the resulting αCT-αCT derivatives on nAChR preparations. Complementary data were obtained from the analysis of a covalent heteromeric dimer, composed of α-cobratoxin and cytotoxin 3 (αCT-CTX).

## EXPERIMENTAL PROCEDURES

*Isolation of Dimers*—αCT-αCT and α-CT-CTX were purified as in Ref. 7.

*Crystallization and X-ray Analysis*—The lyophilized αCT-αCT homodimer was resuspended in water to a concentration of 5 mg/ml and crystallized using the vapor diffusion method by mixing the toxin in a 1:1 ratio with the reservoir solution composed of 60% (v/v) 2-methyl-2,4-pentanediol and 0.1 M glycine-HCl buffer at pH 2. Crystals were flash frozen in liquid nitrogen prior to data collection. The αCT-αCT dimer crystallized in space group $P3_121$ with parameters described in Table 1. Data were collected at 100 K on beamline ID14-EH1 at the ESRF (Grenoble, France) and were processed using XDS and scaled with XSCALE (8, 9). Monomeric α-CT (Protein Data Bank (PDB) code 2CTX) (10) was used as model in molecular replacement trials using Phaser (11) as implemented in the CCP4 software suite (12). Automatic model building was performed using ArpWarp (13). Iterative rounds of manual structure building and refinement were carried out using COOT (14) and REFMAC (15). The first 67 residues of the toxin were well defined in electron density whereas the last 4 could not be built and are likely to be flexible. The final structure (Fig. 1) was validated using the Molprobity server (16). Superpositions were performed using SSM (17), and figures were generated using PyMOL.

**TABLE 1**
**Crystallographic data and refinement parameters**

| | |
|---|---|
| **Crystal parameters** | |
| Space group | $P3_121$ |
| Cell dimensions | |
| *a*, *b* (Å) | 86.00 |
| *c* (Å) | 37.12 |
| α, β, γ (°) | 90, 90, 120 |
| **Data collection** | |
| Resolution range(Å) | 16.33–1.94 (2.04–1.94) |
| $R_{merge}$ (%) | 17.6 (65.5) |
| $I/\sigma I$ | 10.19 (2.78) |
| Completeness (%) | 100 (100) |
| Redundancy | 5.0 (4.9) |
| **Refinement statistics** | |
| Resolution (Å) | 37.24–1.94 |
| No. reflections | 11,874 |
| $R_{work}$/ $R_{free}$ | 0.21/0.25 |
| No. atoms | |
| Protein | 1,009 |
| Ligand/ion | 8 |
| Water | 69 |
| *B*-factors | |
| Protein | 39.7 |
| Ligand/ion | 46.2 |
| Water | 25.8 |
| Root mean square deviations | |
| Bond lengths (Å) | 0.006 |
| Bond angles (°) | 1.053 |

In the crystal structure, two protomers, chains A and B, are present in the asymmetric unit, but these are from two different dimer molecules and share only 183 $Å^2$ at their interface. Each chain makes a dimer with a protomer that is related by a 2-fold crystallographic axis. Hence, chains A and A′, or B and B′ related by the symmetry operation ($-x$, $-x+y$, $-z+1/3$), make up αCT-αCT dimers, which share an interface of ~1400 $Å^2$. The structure of the αCT-αCT dimer has been deposited in the PDB with accession code 4AEA.

*Selective Reduction and Alkylation*—10 nmol of αCT-αCT were dissolved in 50 μl of 50 mM Tris-HCl buffer, pH 8.0, and stirred with 5.5 μl of 2 mM tris(2-carboxyethyl)phosphine (Sigma) under nitrogen for 20 min, then 1 mg of iodoacetamide (Merck) was added under nitrogen for 2 h. The reaction was stopped by direct application on a Phenomenex C18 Jupiter (4.6 × 250 mm) column with subsequent separation of products in a gradient of 15–45% acetonitrile in 30 min in the presence of 0.1% trifluoroacetic acid, at a flow rate of 1.0 ml/min (Fig. 2). Each isolated product underwent rechromatography under the same conditions. Incorporation of amidoethyl groups was checked by MALDI-TOF MS and tandem MS as in Ref. 7.

*Radioligand Analysis*—Competition binding assays (Fig. 3) were carried out using suspensions of nAChR-rich membranes

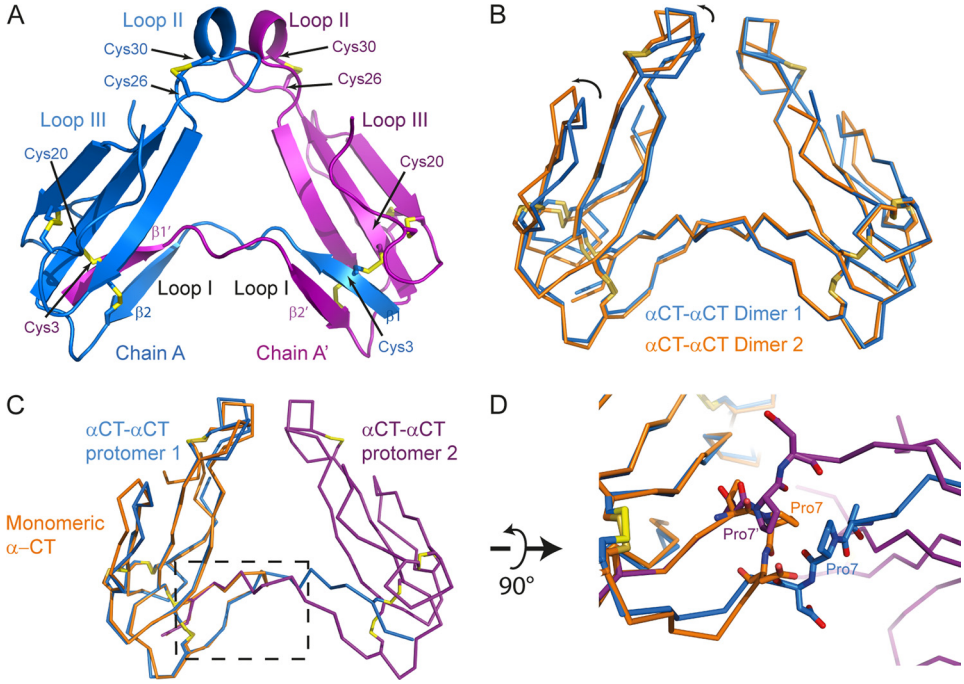


FIGURE 1. **X-ray structure of dimeric αCT.** *A*, αCT-αCT dimer is composed of two protomers represented in *blue* and *purple*, respectively. The β1 strand from the first protomer is extended away from the toxin core and swapped with the β1 strand from the second protomer. Disulfide bridges between $Cys^3$ from one protomer and $Cys^{20}$ from the second protomer stabilize the dimeric toxin. *B*, *ribbon* representation of two αCT-αCT dimers, reconstituted from our structural data, superposed with respect to one of the protomers. The variability between the two dimers likely reflects the flexibility between the two toxin cores. *C*, *ribbon* representation of the superposition of monomeric αCT in *orange* on a protomer of the dimeric αCT (*blue* and *purple*). The *boxed* region is a zoomed in view rotated 90° around a *horizontal axis* in *D*. $Pro^7$ from monomeric αCT (in *orange*) or from either protomer of the αCT-αCT dimer (*blue* and *purple*) is depicted as *sticks*. In the dimeric form, the $Pro^7$ is extended away from the toxin core whereas in the monomeric αCT, $Pro^7$ makes a turn.

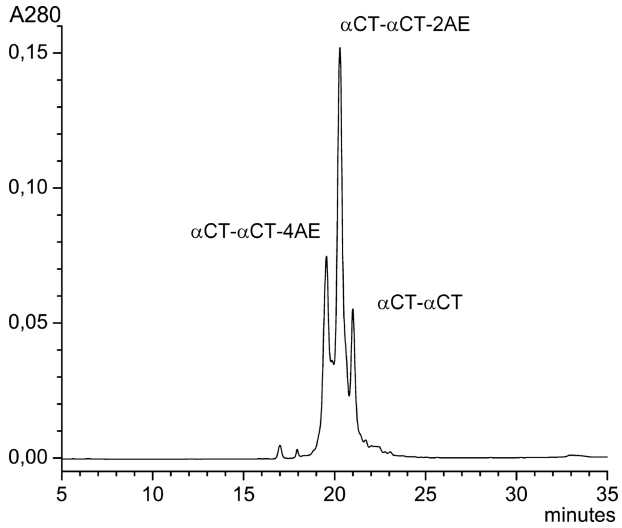


FIGURE 2. **Isolation of αCT dimer derivatives with selectively reduced and alkylated disulfide bonds.** Separation conditions are described under "Experimental Procedures." αCT-αCT-2AE indicates the peak corresponding to dimer with one reduced and aminoethylated disulfide bond, αCT-αCT-4AE is with two reduced and aminoethylated disulfides.

from electric organ *Torpedo californica*, or human α7 nAChR-transfected GH4C1 cells, or *Lymnea stagnalis* or *Aplysia californica* acetylcholine-binding proteins (AChBPs) expressed and purified from baculovirus infected Sf9 cells (18), using $^{125}$I-labeled α-bungarotoxin as reported previously (19).

*Electrophysiological Experiments*—All experiments were conducted at human nAChRs expressed in *Xenopus* oocytes. cDNAs encoding for the α7 or α3 and β2 subunits were injected into the oocyte nucleus using a roboinject (Multichannel Systems, Reutlingen, Germany). cDNA concentrations and injection procedures were standard and as described previously (7). Two to 3 days after injection, recordings were carried out with a two-electrode voltage clamp system using a HiClamp (Multichannel Systems). This system offers the advantage of minimal solution sample and multiple recordings from the same solutions.

*Molecular Modeling*—The refined x-ray structure of dimeric toxin was equilibrated in GROMACS 4.0.3. All molecular simulations were performed in an OPLS-AA force field, and molecular dynamics simulations were calculated at a temperature of 300 K with a dielectric permittivity $\epsilon = 1$. Integration procedures were performed with time steps as small as 1 fs, for simulation times of 20 ns. After molecular dynamics simulations of the energy-minimized αCT-αCT x-ray structure, the obtained molecule was docked to *L. stagnalis* AChBP (*Ls*AChBP) (20). Hex 6.0 was used for docking, and subsequent visual analysis in the SPDBViewer allowed us to reject false positive solutions.

## RESULTS

*Structure of α-CT Dimer*—We have solved the three-dimensional structure of αCT-αCT, a dimeric αCT, at a resolution of 1.94 Å. Within this dimer, protomers are covalently linked by disulfide bonds between $Cys^3$ in one protomer and $Cys^{20}$ in the other, and vice versa (Fig. 1*A*). The two dimers that we reconstituted from our structural data display a slight variation in the relative arrangement of the two protomers around the 2-fold crystallographic axis (Fig. 1*B*), likely reflecting the degree of flexibility of the protomers around this hinge region.

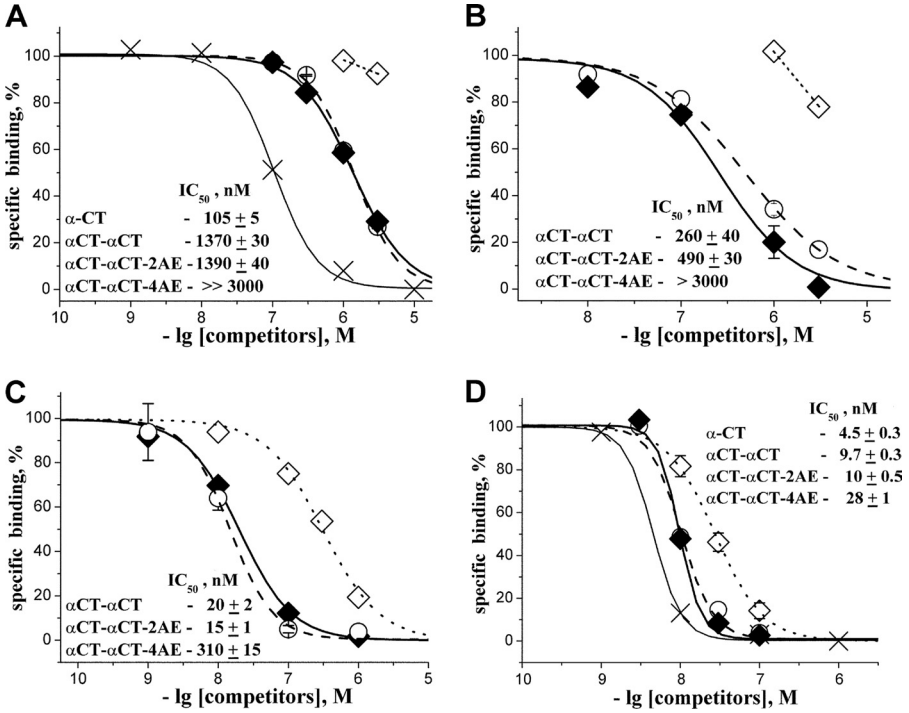


FIGURE 3. **Competition experiments with $^{125}$I-labeled α-bungarotoxin.** Inhibition of radioactive α-bungarotoxin binding to α7 nAChR (*A*), AChBP from *A. californica* (*B*), and *L. stagnalis* (*C*) as well as to *Torpedo* nAChR (*D*) by αCT (×), αCT-αCT (♦),αCT-αCT-2AE (○), and αCT-αCT-4AE (◇) is shown.

The three-dimensional structure of protomers in the dimeric αCT resembles the monomeric αCT (PDB code 2CTX) (10) and essentially preserves the TFT fold, except for a kink at Pro$^7$ (Fig. 1, *C* and *D*). This results in a swap of the first N-terminal β strand from one protomer with that of the second protomer, hence forming the αCT-αCT dimer (Fig. 1*A*). The two αCT protomers are related by a 2-fold axial symmetry. Whereas in monomeric αCT the N-terminal β strand is arranged in an antiparallel manner with respect to the second N-terminal β strand through a turn induced by Pro$^7$, in the dimeric αCT-αCT this Pro$^7$ is not involved in generating a turn but allows the outward extension of the first N-terminal β strand away from the toxin core. The extended β1 strand displays a large interaction interface with the β2 strand from the second protomer contributing to the dimeric αCT-αCT. These two N-terminal β strands are covalently linked through two disulfide bridges: Cys$^3$ of each chain is bound to Cys$^{20}$ of the other chain (Cys$^3$-Cys$^{20'}$ and Cys$^{3'}$-Cys$^{20}$). Interestingly, these cysteine residues are highly conserved in α-neurotoxins and are involved in an internal disulfide bond in monomeric αCT. However, reduction of these disulfides in κ-bungarotoxin did not considerably decrease toxin activity against α3β2 nAChRs (21). Even such a drastic disulfide bond rearrangement as observed in the αCT-αCT does not affect the three-finger motif in each of the polypeptide chains of the protomers. Indeed, a protomer of αCT-αCT superposes on the monomeric αCT with a root mean square deviation of 0.9 Å (over residues 9–67) (Fig. 1*C*). The first loops of the protomers are maintained through the β strand swap between the two protomers constituting the covalent dimer (Fig. 1*A*). The geometry of all other disulfide bridges in both polypeptide chains of αCT-αCT is similar to that observed in monomeric αCT. The interface between the two protomers of the covalent dimer extends over ~1400 Å$^2$, with the tip of loops II contributing ~440 Å$^2$, and involves 42 hydrogen bonds between the two polypeptide chains as characterized by the PISA server (22).

*Alkylation of Additional Disulfides in αCT Dimer*—The loop II additional disulfide in long chain α-neurotoxins is crucial for the interaction with α7 nAChR (4). We wondered whether this loop II disulfide bridge is important for dimeric αCT function and used the fact that it can be selectively reduced and alkylated (23, 24). These loop II additional disulfides are exposed in the structure and are therefore accessible to selective reduction and subsequent alkylation, in contrast to other intramolecular or intermolecular disulfide bridges of the toxin. We have generated αCT-αCT derivatives where this disulfide bond (Cys$^{26}$-Cys$^{30}$) has been reduced and ethylamidated (Fig. 2). This reaction appears to be kinetically controlled, similarly to what is observed with αCT (24) and does not disrupt the dimeric structure of αCT-αCT. Interestingly, under chosen conditions the loop II disulfide bridges from each protomer can be reduced simultaneously, and the reaction mixture contains derivatives with either a single reduced and alkylated disulfide (αCT-αCT-2AE), or with both disulfides modified (αCT-αCT-4AE). This is in agreement with our earlier isolation both of the 24–33 tryptic peptide fragment of the loop II, containing two pyridylethyl groups, and of the same peptide with the intact disulfide bond (7). Fortunately, it was possible to separate the two different derivatives from each other and from the parent molecule (Fig. 2) for further analysis of their biological activity.

*Competition Experiments with $^{125}$I-Labeled α-Bungarotoxin*—Disturbing the central loop II structure in both protomers by

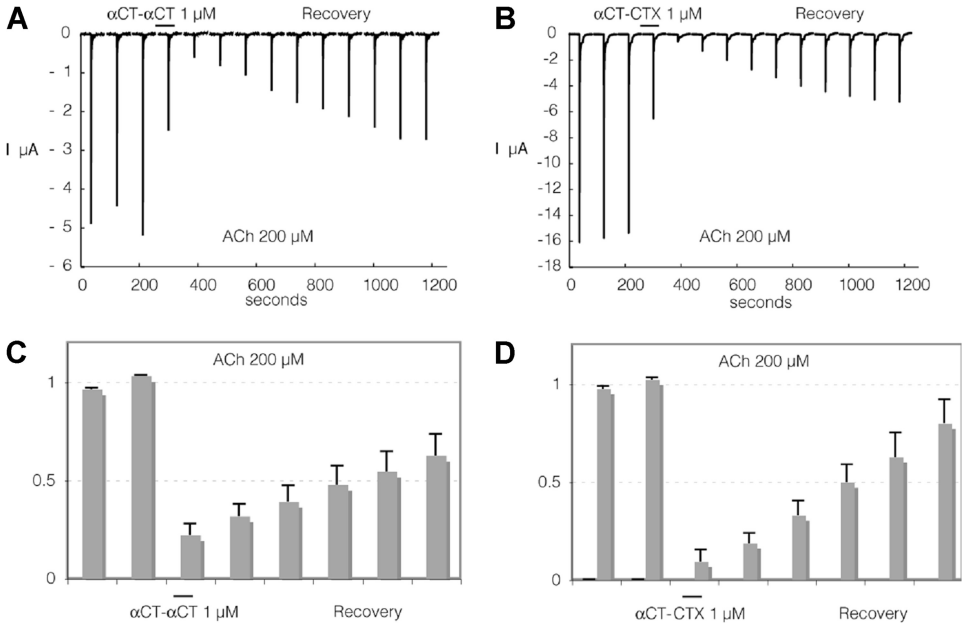


FIGURE 4. **Interaction of αCT-αCT and of heterodimer αCT-CTX with human α7nAChR heterologously expressed in *Xenopus* oocytes.** To evaluate effects of the toxin, cells were challenged at a regular interval (2 min) with brief ACh test pulses (200 μM, 5 s). Following a stabilization period, toxin was applied at 1 μM for at least 1 min. The response to ACh (200 μM) was tested again, and recovery from inhibition was monitored over several minutes. Results obtained with αCT-αCT are illustrated in *A* and *C* whereas effects of αCT-CTX are shown in *B* and *D*. Average effects of αCT-αCT measured on three cells with 10-min recovery are presented in *C*. Average effects of αCT-CTX are presented in *D* on four cells. *Bars* indicate S.E.

reducing the additional disulfides and alkylating the respective cysteine residues results in a significant decrease in affinity of the modified αCT-αCT both for the α7 nAChR (Fig. 3*A*) and for AChBPs (Fig. 3, *B* and *C*), soluble structural homologs of the nAChR ligand binding domains (20). However, if only one of the loop II disulfide bridges in the αCT-αCT is disrupted, the affinity remains virtually unchanged (Fig. 3, *A*–*C*). This suggests that preserving the native structure in only one of the central loops II of the dimer is sufficient for effective interaction of αCT-αCT with these targets.

Nevertheless, as might be expected, reduction of one or both these disulfides in αCT-αCT does not practically affect its interaction with the muscle-type nAChR (Fig. 3*D*), similar to what was observed for the interaction with this receptor following the reduction of the loop II disulfide bridge in αCT (4)

*Electrophysiology Studies*—The activity of αCT-αCT and its reduced derivatives was compared at human α7 and α3β2 nAChRs expressed in *Xenopus* oocytes. Because naturally occurring dimers αCT-αCT and αCT-CTX and especially individual reduced/alkylated derivatives of the former dimer were available only in minor amounts, we could not characterize the results of the electrophysiological experiments in terms of $IC_{50}$ as was done in the above described competition binding experiments. In view of the latter, all dimers were applied at 1 μM concentration, and their inhibitory activity is illustrated by Figs. 4–7 representing a decrease in the amplitude of the acetylcholine-induced currents from 10 to 90%.

Similar to the results of binding studies, reduction of only one disulfide in αCT-αCT practically does not decrease the inhibitory activity against α7 nAChR, but it drops considerably if both disulfides are reduced and alkylated (compare Fig. 4*A* with Fig. 5, *A* and *B*). Surprisingly, with the α3β2 nAChR both αCT-αCT derivatives have a very similar activity which is much higher than that of αCT-αCT itself (compare Fig. 6, *A*–*D*, with Fig. 7, *A* and *C*). Interestingly, for the heterodimer αCT-CTX which showed quite potent inhibition of $^{125}$I-labeled α-bungarotoxin binding to α7 nAChR (7), in the present electrophysiology experiments we found that this protein is not only slightly more active than αCT-αCT in inhibiting α7 nAChR (compare Fig. 4, *A* and *C*, with Fig. 4, *B* and *D*), but considerably exceeds the αCT-αCT homodimer in blocking the α3β2 nAChR (Fig. 7).

*Computer Modeling*—Superposition of one protomer of the αCT-αCT dimer onto monomeric αCT bound to *Ls*AChBP (PDB code 1YI5) (20) (Fig. 8*A*) reveals that such an interaction would be energetically unfavorable due to a very close disposition of the loop II tips from the two protomers leading to clashes between the second αCT-αCT protomer and *Ls*AChBP. To identify potential conformational changes in the dimeric toxin likely to lead to binding to AChBP, we performed molecular dynamics simulation trials followed by docking to *Ls*AChBP. Our results suggest that a rotation around the Pro$^7$-Asp$^8$ bonds from both protomers could provide conformations (Fig. 8*B*) that are likely to be energetically more favorable for the complex formation (Fig. 8*C*) and which would resemble those of κ-bungarotoxin (Fig. 9*B*) or haditoxin (Fig. 9*C*).

## DISCUSSION

Our 1.94 Å resolution x-ray structure of αCT-αCT, a covalently linked dimer of αCT isolated earlier from the *N. kaouthia* cobra venom (7), reveals how the two protomers composing the toxin are bridged and how they are oriented relative to each other (Fig. 1*A*). It shows that two interchain disulfide bonds connect the interweaved loops I of the two monomeric αCT, namely Cys$^3$ of one monomer is bound to Cys$^{20}$ of the second monomer and vice versa. Each protomer essentially preserves a

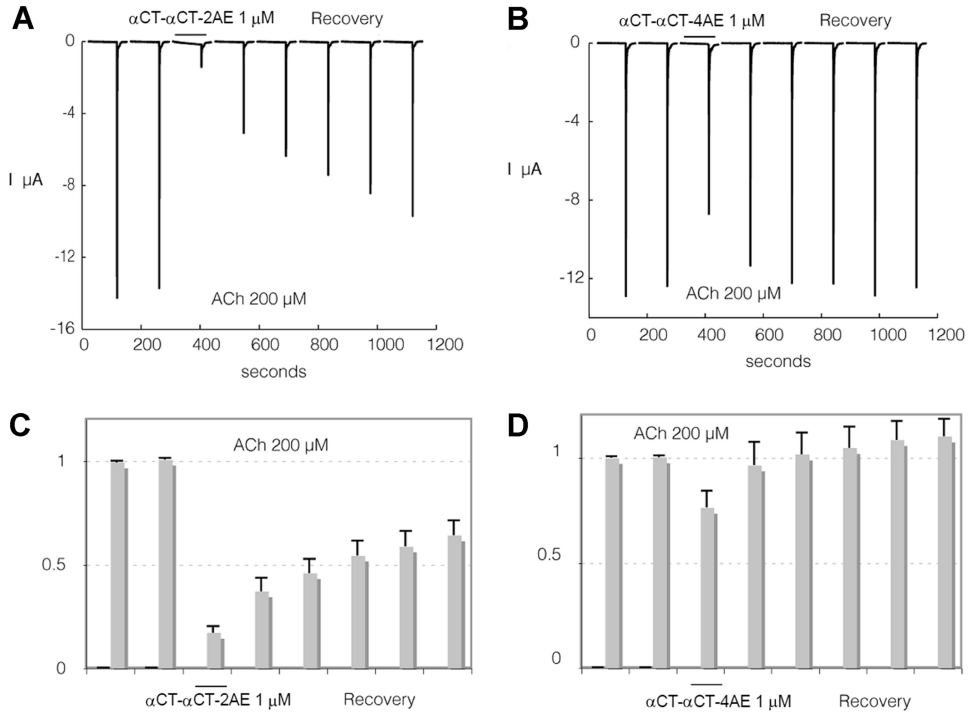


FIGURE 5. **Interaction of αCT-αCT reduced and alkylated derivatives with human α7nAChR heterologously expressed in *Xenopus* oocytes.** To evaluate effects of the toxin, cells were challenged at a regular interval (2 min) with brief ACh test pulses (200 μM, 5 s). Following a stabilization period, toxin was applied at 1 μM for at least 1 min. The response to ACh (200 μM) was tested again, and recovery from inhibition was monitored over several minutes. Results obtained with αCT-αCT-2AE are illustrated in *A* and *C*, whereas effects of αCT-CT-4AE are shown in *B* and *D*. Average effects of αCT-αCT-2AE measured on four cells with 10-min recovery are presented in *C*. Average effects of αCT-αCT-4AE on four cells are presented in *D*. *Bars* indicate S.E.

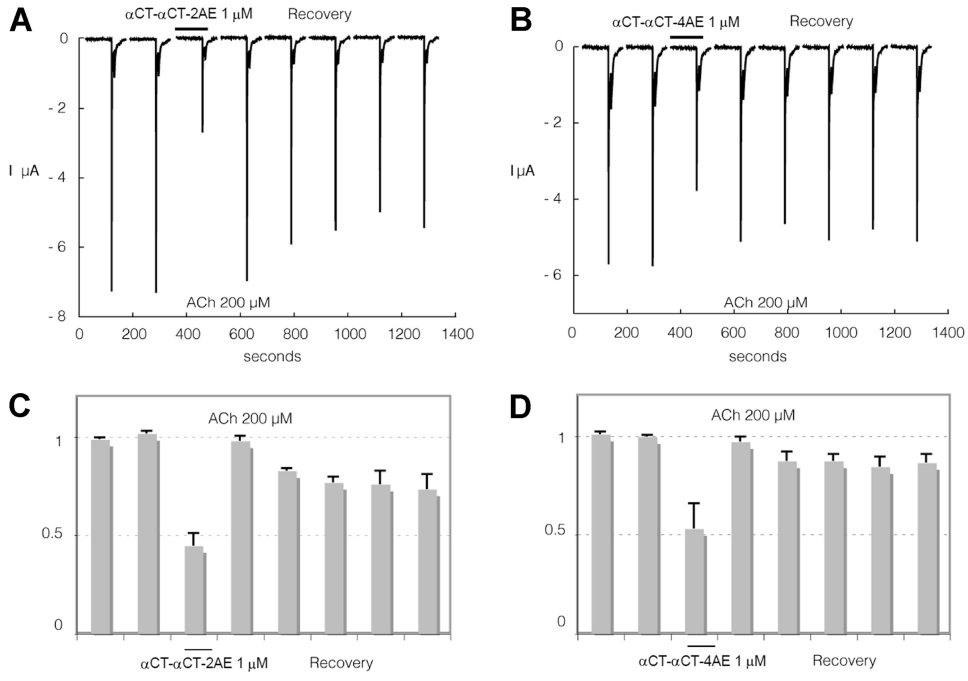


FIGURE 6. **Interaction of αCT-αCT reduced and alkylated derivatives with human α3β2 nAChR heterologously expressed in *Xenopus* oocytes.** Experiments were carried out at cells expressing the human α3β2 nAChRs using the same experimental protocol as in Fig. 4. *C* and *D* illustrate average values recorded at four and five cells, respectively. *Bars* indicate S.E.

three-finger fold, as suggested from earlier circular dichroism experiments (7), whereas the overall three-dimensional structure shows that the loop II tips of each protomer of the αCT-αCT are in close proximity to each other. The current lack of structural data for complexes of dimeric TFTs with AChBPs, nAChRs, or with their ligand-binding domains hinders the rationalization of differences in the interactions of αCT-αCT, its reduced derivatives, and of a heterodimeric αCT-CTX with distinct nAChR subtypes. Superposing the αCT-αCT structure on that of monomeric αCT in complex with *Ls*AChBP (26) (Fig.

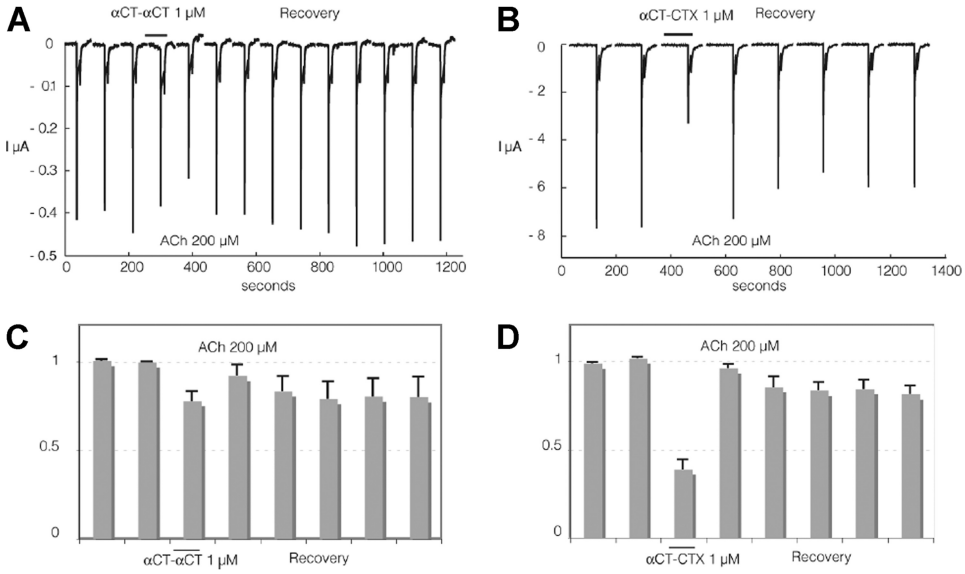


FIGURE 7. **Interaction of αCT-αCT and of heterodimer αCT-CTX with human α3β2 nAChR heterologously expressed in *Xenopus* oocytes.** Experiments were carried out at cells expressing the human α3β2 nAChRs using the same experimental protocol as in Fig. 4. *C* and *D* illustrate average values recorded at six and five cells, respectively. *Bars* indicate S.E.

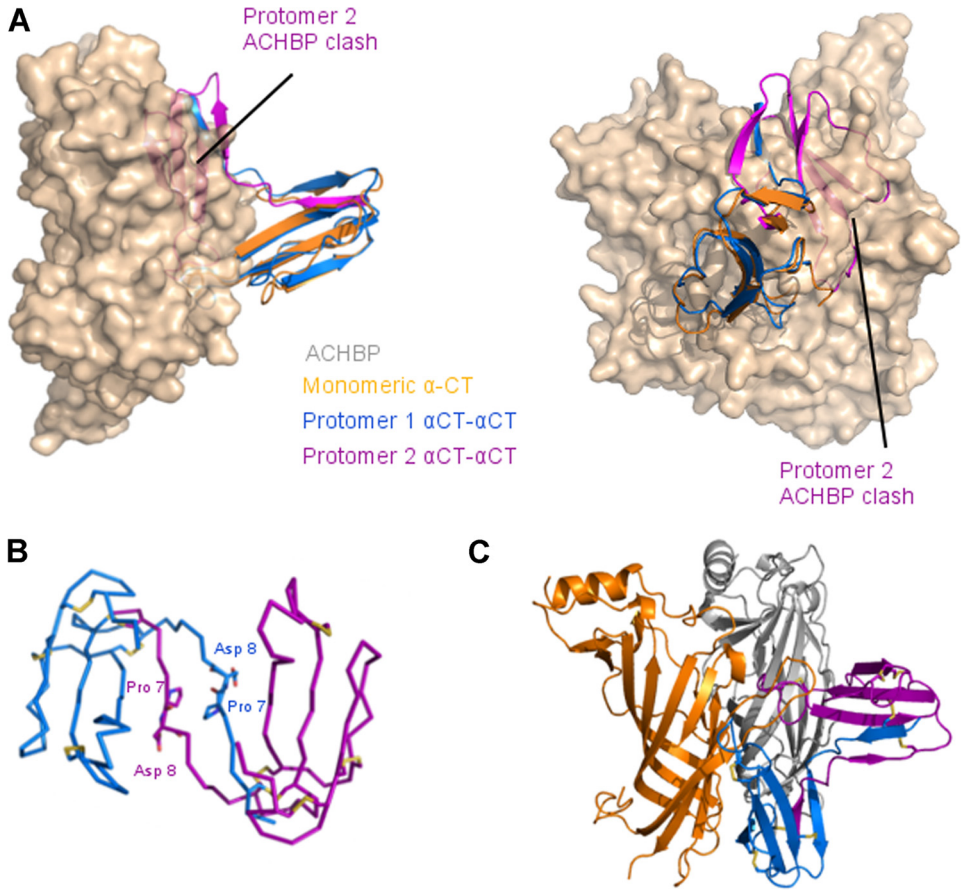


FIGURE 8. *A*, superposition of a protomer of αCT-αCT (*blue* and *purple*) onto monomeric αCT (*orange*) in complex with *Ls*AChBP (PDB code 1YI5) (surface representation, *colored silicon* of one AChBP protomer-protomer interface). A single monomeric αCT is shown bound to *Ls*AChBP for clarity. *B*, *ribbon* representation of an αCT-αCT model obtained after molecular dynamics simulations. $Pro^{7}$ and $Asn^{8}$ are shown as *sticks* in each protomer. *C*, scheme of possible binding mode of αCT-αCT to *Ls*AChBP.

8) suggests that binding to receptors would be energetically unfavorable. In this configuration, the interaction of one αCT-αCT protomer with the receptor ligand binding domain would lead to steric clashes of the second protomer with the receptor (Fig. 8*A*). Indeed, for αCT-αCT to interact with the receptor, a conformational change inducing a relative reorientation of the loops II of the two protomers would be required (Fig. 8*B*). Interestingly, the spectrum of αCT-αCT activity toward distinct nic-

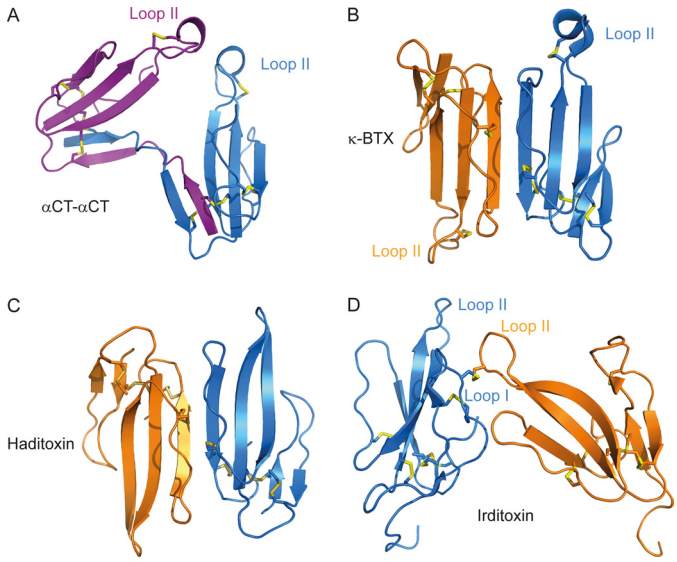


FIGURE 9. **Schematic representations of αCT-αCT (*A*), noncovalent dimeric toxins κ-bungarotoxin (κ-*BTX*) (*B*) and haditoxin (*C*), and irditoxin, a covalent dimer (*D*).** In the κ-bungarotoxin dimer the β strands from the two protomers constitute an extended antiparallel β sheet, with the loop II from each subunit oriented in opposite directions. A similar topological arrangement is observed for haditoxin. A disulfide bridge is formed between the two irditoxin protomers, involving a loop I cysteine from the first chain (*blue*) and a loop II cysteine from the second chain (*orange*). Contrary to κ-bungarotoxin or haditoxin, but similar to the αCT-αCT dimer, the loops II from the two protomers are oriented toward each other.

otinic receptors is different from what is observed with the monomeric αCT. The dimeric αCT-αCT is able to bind to the muscle-type and α7 nAChRs, but in contrast to monomeric αCT it can also block the heteromeric α3β2 nAChR (7). Because in this activity it resembles κ-bungarotoxin, a noncovalent dimer (27), it is possible that dimerization is a requirement for the binding of a TFT to heteromeric α3β2 nAChRs.

κ-Bungarotoxins are noncovalent TFT dimers from krait venoms structurally related to long chain α-neurotoxins. They block heteromeric α3β2 and bind weakly to α4β2 and α7 nAChRs (7, 27). κ-Bungarotoxin forms a dimer related by a planar rotation of ~180° (Fig. 9*B*) bringing the three-stranded β sheets in each protomer to form an extended six-stranded antiparallel β sheet in the dimer, with a 493 Å$^2$ interaction surface (5). Interestingly, from the crystal structures of αCT (PDB code 2CTX) (10) or of α-bungarotoxin (PDB code 1HC9) (28), the interactions between symmetry-related monomers result in a dimer arrangement very similar to that observed for κ-bungarotoxin.

After our discovery of the dimeric α-cobratoxin (7), two novel dimeric three-finger neurotoxins have been described, namely irditoxin from *Boiga irregularis* venom (29) and haditoxin from the king cobra (30). Haditoxin is a noncovalent dimer composed of two short chain α-neurotoxins and adopts a topological arrangement (Fig. 9*C*) reminiscent of that observed for κ-bungarotoxin, on which it superposes with a root mean square deviation of 2 Å. It also displays a protomer-protomer interaction surface of 570 Å$^2$, comparable with that between the protomers of the κ-bungarotoxin dimer. Haditoxin can block not only muscle-type nAChRs, as typically observed for short chain α-neurotoxins, but unexpectedly also blocks homomeric α7 and heteromeric α3β2 nAChRs. This confirms our earlier conclusion that dimerization resulting in noncovalently or in covalently linked TFTs is an important factor for recognition of heteromeric nAChRs (7). Haditoxin does not comprise an additional loop II disulfide, and its activity raises the question about the role of such a disulfide in recognition of neuronal nAChRs. Nevertheless, it should be kept in mind that blocking of neuronal nAChRs by haditoxin was only observed at very high toxin concentrations (30). The monomeric form of haditoxin has not been isolated and cannot be used for comparison purposes, contrary to the αCT-αCT dimer where the activity of αCT is well characterized and overlaps considerably with that of the covalently bound dimer. Furthermore, the classification of haditoxin to the family of short α-neurotoxins is controversial since its homology to erabutoxin, a classical short chain α-neurotoxin, is only 50%, whereas it is of 75–80% with the muscarinic toxin-like proteins, which are of different origin (25).

Irditoxin, yet another recently described dimeric toxin, consists of two highly homologous "weak" or "nonconventional" toxin-like protomers linked through a disulfide bridge and is selective for bird muscle-type nAChR (29). Each of these two protomers contains one additional cysteine residue (absent in typical TFTs), which covalently link the two irditoxin protomers via an intermolecular disulfide bridge. In the first chain, the additional cysteine is located in loop I whereas it is in loop II in the second chain. The three-dimensional structure of irditoxin (29) (Fig. 9*D*) shows that loops II of the two protomers are oriented in a somewhat similar way as those of the αCT-αCT dimer (Fig. 9*A*). In the case of irditoxin, however, a much smaller interaction surface is shared by the two protomers (~430 Å$^2$ against ~1400 Å$^2$ in αCT-αCT).

Considering the importance of the additional loop II disulfide bridge for αCT interaction with the α7 nAChR (4) and for κ-bungarotoxin binding to α3β2 nAChR (27), we characterized the role of this disulfide in αCT-αCT interaction with different targets, namely with several subtypes of nAChRs and with AChBPs. Toward this end, we alkylated αCT-αCT using iodoacetamide, which does not significantly contribute to the molecular charge or to the molecular mass of the dimer. Our binding (Fig. 3) and electrophysiology data (Figs. 4–6) show that the presence of an additional disulfide in only one of the two loops II of the dimer is sufficient for the interaction with both α7 nAChR and AChBPs. However, both disulfides can be reduced and alkylated without diminishing the efficiency of binding to the muscle-type nAChR (Fig. 3*D*). Thus, our binding and electrophysiology data on the interaction of αCT-αCT with the α7 and muscle-type nAChRs correlate well with previous data on monomeric αCT concerning the role of the disulfide bridge in the central loop II. However, in contrast to what is known for the κ-bungarotoxin noncovalent dimer, loop II disulfides in αCT-αCT are not essential for interaction with the α3β2 nAChR. On the contrary, reduction and alkylation of one or both of those disulfide bridges considerably enhance the inhibitory activity of the toxin variant against the α3β2 nAChR (Figs. 6 and 7).

The opposite roles of the central loop II disulfides in the interaction of dimeric TFTs with the α7 nAChR compared with the α3β2 nAChR are also illustrated by our results for the αCT-

CTX heterodimer composed of α-cobratoxin and cytotoxin 3. The cytotoxin in this heterodimeric toxin is a short type TFT and contains no additional disulfide bridge in the loop II. However, the presence of a single loop II disulfide bridge in the αCT protomer within the αCT-CTX heterodimer is sufficient for blocking the α7 nAChR at least as efficiently as does αCT-αCT (Fig. 4, *A* and B). Moreover, this heterodimer is more potent than αCT-αCT against the α3β2 nAChR (Fig. 7). These results confirm and extend our earlier conclusion that dimerization is essential for the activity of TFTs against heteromeric neuronal nAChRs. Our data for the reduced derivatives of αCT-αCT, as well as literature data for haditoxin (30), also show that α3β2 nAChRs can be recognized by dimeric TFTs containing no additional disulfides in the loops II. αCT-αCT, in which one of the additional disulfides is preserved, appears to be more active against α3β2 nAChR than αCT-αCT in which these both disulfides are disrupted (Fig. 6, *C* and *D*) and comparable with the heterodimer that has also only one such disulfide (Fig. 7, *B* and *D*).

In summary, we have determined the x-ray structure of αCT-αCT, a covalent αCT dimer, and found that the dimerization results from a β strand swap between the two protomers, two covalent linkages arising between $Cys^3$ of one protomer and $Cys^{20}$ of the second, and vice versa. We also investigated how specific αCT-αCT binding is to different nAChR subtypes and how effective the dimeric toxin is at blocking these receptors. Our data confirm that dimerization is an important prerequisite for TFT interaction with heteromeric neuronal nAChRs, and from comparison of our and literature data it follows that the receptor recognition is possible with different relative orientations of protomers in the TFT dimers. We further find that at least one loop II disulfide bridge is required for activity against the α7 nAChR, whereas the reduction of one or both loop II disulfide bridges potentiates the activity of the dimeric toxin against the heteromeric α3β2 nAChR.

*Acknowledgment—We thank the ESRF ID14-EH1 beamline scientists for assistance during data collection.*

## REFERENCES


1. Gotti, C., Moretti, M., Gaimarri, A., Zanardi, A., Clementi, F., and Zoli, M. (2007) Heterogeneity and complexity of native brain nicotinic receptors. *Biochem. Pharmacol.* **74,** 1102–1111
2. de Jonge, W. J., and Ulloa, L. (2007) The α7 nicotinic acetylcholine receptor as a pharmacological target for inflammation. *Br. J. Pharmacol.* **151,** 915–929
3. Tsetlin, V. (1999) Snake venom α-neurotoxins and other "three-finger" proteins. *Eur. J. Biochem.* **264,** 281–286
4. Antil-Delbeke, S., Gaillard, C., Tamiya, T., Corringer, P. J., Changeux, J. P., Servent, D., and Ménez, A. (2000) Molecular determinants by which a long chain toxin from snake venom interacts with the neuronal α7-nicotinic acetylcholine receptor. *J. Biol. Chem.* **275,** 29594–29601
5. Oswald, R. E., Sutcliffe, M. J., Bamberger, M., Loring, R. H., Braswell, E., and Dobson, C. M. (1991) Solution structure of neuronal bungarotoxin determined by two-dimensional NMR spectroscopy: sequence-specific assignments, secondary structure, and dimer formation. *Biochemistry* **30,** 4901–4909
6. Mordvintsev, D. Y., Polyak, Y. L., Rodionov, D. I., Jakubik, J., Dolezal, V., Karlsson, E., Tsetlin, V. I., and Utkin, Y. N. (2009) Weak toxin WTX from *Naja kaouthia* cobra venom interacts with both nicotinic and muscarinic acetylcholine receptors. *FEBS J.* **276,** 5065–5075
7. Osipov, A. V., Kasheverov, I. E., Makarova, Y. V., Starkov, V. G., Vorontsova, O. V., Ziganshin, R. K., Andreeva, T. V., Serebryakova, M. V., Benoit, A., Hogg, R. C., Bertrand, D., Tsetlin, V. I., and Utkin, Y. N. (2008) Naturally occurring disulfide-bound dimers of three-fingered toxins: a paradigm for biological activity diversification. *J. Biol. Chem.* **283,** 14571–14580
8. Kabsch, W. (2010) XDS. *Acta Crystallogr. D Biol. Crystallogr.* **66,** 125–132
9. Kabsch, W. (2010) Integration, scaling, space-group assignment, and post-refinement. *Acta Crystallogr. D Biol. Crystallogr.* **66,** 133–144
10. Betzel, C., Lange, G., Pal, G. P., Wilson, K. S., Maelicke, A., and Saenger, W. (1991) The refined crystal structure of α-cobratoxin from *Naja naja siamensis* at 2.4-A resolution. *J. Biol. Chem.* **266,** 21530–21536
11. McCoy, A. J., Grosse-Kunstleve, R. W., Adams, P. D., Winn, M. D., Storoni, L. C., and Read, R. J. (2007) Phaser crystallographic software. *J. Appl. Crystallogr.* **40,** 658–674
12. Collaborative Computational Project, Number 4 (1994) The CCP4 suite: programs for protein crystallography. *Acta Crystallogr. D Biol. Crystallogr.* **50,** 760–763
13. Langer, G., Cohen, S. X., Lamzin, V. S., and Perrakis, A. (2008) Automated macromolecular model building for X-ray crystallography using ARP/wARP version 7. *Nat. Protoc.* **3,** 1171–1179
14. Emsley, P., Lohkamp, B., Scott, W. G., and Cowtan, K. (2010) Features and development of COOT. *Acta Crystallogr. D Biol. Crystallogr.* **66,** 486–501
15. Murshudov, G. N., Vagin, A. A., and Dodson, E. J. (1997) Refinement of macromolecular structures by the maximum-likelihood method. *Acta Crystallogr. D Biol. Crystallogr.* **53,** 240–255
16. Chen, V. B., Arendall, W. B., 3rd, Headd, J. J., Keedy, D. A., Immormino, R. M., Kapral, G. J., Murray, L. W., Richardson, J. S., and Richardson, D. C. (2010) MolProbity: all-atom structure validation for macromolecular crystallography. *Acta Crystallogr. D Biol. Crystallogr.* **66,** 12–21
17. Krissinel, E., and Henrick, K. (2004) Secondary-structure matching (SSM), a new tool for fast protein structure alignment in three dimensions. *Acta Crystallogr. D Biol. Crystallogr.* **60,** 2256–2268
18. Celie, P. H., van Rossum-Fikkert, S. E., van Dijk, W. J., Brejc, K., Smit, A. B., and Sixma, T. K. (2004) Nicotine and carbamylcholine binding to nicotinic acetylcholine receptors as studied in AChBP crystal structures. *Neuron* **41,** 907–914
19. Kasheverov, I. E., Zhmak, M. N., Fish, A., Rucktooa, P., Khruschov, A. Y., Osipov, A. V., Ziganshin, R. H., D'hoedt, D., Bertrand, D., Sixma, T. K., Smit, A. B., and Tsetlin, V. I. (2009) Interaction of α-conotoxin ImII and its analogs with nicotinic receptors and acetylcholine-binding proteins: additional binding sites on *Torpedo* receptor. *J. Neurochem.* **111,** 934–944
20. Brejc, K., van Dijk, W. J., Klaassen, R. V., Schuurmans, M., van Der Oost, J., Smit, A. B., and Sixma, T. K. (2001) Crystal structure of an ACh-binding protein reveals the ligand-binding domain of nicotinic receptors. *Nature* **411,** 269–276
21. Grant, G. A., Luetje, C. W., Summers, R., and Xu, X. L. (1998) Differential roles for disulfide bonds in the structural integrity and biological activity of κ-bungarotoxin, a neuronal nicotinic acetylcholine receptor antagonist. *Biochemistry* **37,** 12166–12171
22. Krissinel, E., and Henrick, K. (2007) Inference of macromolecular assemblies from crystalline state. *J. Mol. Biol.* **372,** 774–797
23. Chicheportiche, R., Vincent, J. P., Kopeyan, C., Schweitz, H., and Lazdunski, M. (1975) Structure-function relationship in the binding of snake neurotoxins to the *Torpedo* membrane receptor. *Biochemistry* **14,** 2081–2091
24. Martin, B. M., Chibber, B. A., and Maelicke, A. (1983) The sites of neurotoxicity in α-cobratoxin. *J. Biol. Chem.* **258,** 8714–8722
25. Kukhtina, V. V., Weise, C., Muranova, T. A., Starkov, V. G., Franke, P., Hucho, F., Wnendt, S., Gillen, C., Tsetlin, V. I., and Utkin, Y. N. (2000) Muscarinic toxin-like proteins from cobra venom. *Eur. J. Biochem.* **267,** 6784–6789
26. Bourne, Y., Talley, T. T., Hansen, S. B., Taylor, P., and Marchot, P. (2005) Crystal structure of a Cbtx-AChBP complex reveals essential interactions between snake α-neurotoxins and nicotinic receptors. *EMBO J.* **24,** 1512–1522

27. Luetje, C. W., Wada, K., Rogers, S., Abramson, S. N., Tsuji, K., Heinemann, S., and Patrick, J. (1990) Neurotoxins distinguish between different neuronal nicotinic acetylcholine receptor subunit combinations. *J. Neurochem.* **55,** 632–640
28. Harel, M., Kasher, R., Nicolas, A., Guss, J. M., Balass, M., Fridkin, M., Smit, A. B., Brejc, K., Sixma, T. K., Katchalski-Katzir, E., Sussman, J. L., and Fuchs, S. (2001) The binding site of acetylcholine receptor as visualized in the x-ray structure of a complex between α-bungarotoxin and a mimotope peptide. *Neuron* **32,** 265–275
29. Pawlak, J., Mackessy, S. P., Sixberry, N. M., Stura, E. A., Le Du, M. H., Ménez, R., Foo, C. S., Ménez, A., Nirthanan, S., and Kini, R. M. (2009) Irditoxin, a novel covalently linked heterodimeric three-finger toxin with high taxon-specific neurotoxicity. *FASEB J.* **23,** 534–545
30. Roy, A., Zhou, X., Chong, M. Z., D'hoedt, D., Foo, C. S., Rajagopalan, N., Nirthanan, S., Bertrand, D., Sivaraman, J., and Kini, R. M. (2010) Structural and functional characterization of a novel homodimeric three-finger neurotoxin from the venom of *Ophiophagus hannah* (king cobra). *J. Biol. Chem.* **285,** 8302–8315